



Performance Characteristics of Horizontal Interlaced Multilayer Moored Floating Pipe Breakwater

A. Vittal Hegde¹; Kiran Kamath²; and Amit S. Magadum³

Abstract: The paper presents the results of model scale experiments for the study of wave attenuation by horizontal interlaced, multilayer, moored floating pipe breakwater. A review of some significant floating breakwater models proposed by earlier investigators is included. For a floating breakwater the transmission coefficient (K_t) is influenced by relative width of the breakwater (W/L). Nondimensional graphs indicating the variation of K_t with respect to W/L (with H_t/L as a parameter for different H_t/d values) and K_t versus H_t/L (for a range of d/L values from 0.09 to 0.24) have been plotted. Further variation of K_t with relative depth d/L for different W/L values is also studied. From the experimental study and results obtained, it is found that the transmission coefficient decreases with an increase in relative breakwater width W/L and wave steepness H_t/L for all H_t/d values. In the present study it was observed that performance was better for breakwater configurations of $W/L \geq 0.7$ when compared with configurations of $W/L < 0.7$. Further, the experimental results obtained were compared with the output of a mathematical model. From the comparison for $H_t/L = 0.04$, values of K_t obtained from the present experiments were in agreement with those obtained from the mathematical model.

DOI: 10.1061/(ASCE)0733-950X(2007)133:4(275)

CE Database subject headings: Floating breakwaters; Model studies; Performance characteristics; Scale models.

Introduction

In the recent years, floating breakwaters have generated a great deal of interest in the field of ocean engineering, as they are less expensive compared to conventional type breakwaters founded on the ocean bed. In addition, they have several desirable characteristics such as comparatively small capital cost, adaptability to varying harbor shapes and sizes, low construction time, and freedom from silting and scouring. Floating breakwaters could also be utilized to meet location changes, extent of protection required, or seasonal demand. They can be used as temporary protection for offshore activities in hostile environments during construction, drilling works, salvage operations, etc.

Invariably, floating breakwaters are conceived based on the concept of either reflecting the wave energy or dissipating wave energy by induced turbulent motion. In recent times, many types of floating breakwater models have been tested and some have been constructed and their prototype performances assessed. Floating breakwaters can be subdivided into four general categories:

Box, pontoon, mat, and tethered float. The prime factor in the construction of the floating breakwaters is to make the width of the breakwater (in the direction of wave propagation) greater than one-half the wavelength and preferably as wide as the incident wavelength; else, the breakwater rides over the top of the wave without attenuating it. Also to be effective, the floating breakwater must be moored in place with both leeward and windward ties; otherwise, it would sag off and ride over the incident wave. Pontoon and box type floating breakwaters belong to the first category in which the wave attenuation is achieved by reflecting the wave energy. Mat and tethered belong to the second category in which wave energy dissipation is mainly due to drag from the resultant motion of the float.

There are four fundamental aspects of floating breakwater design:

1. Buoyancy and floating stability;
2. Wave transmission;
3. Mooring forces; and
4. Breakwater unit structural design.

With regards to buoyancy, a floating breakwater must possess sufficient buoyancy to support the weight of the breakwater and its moorings. The moored breakwater will have, associated with its motion, a natural period of oscillation. It is expected from the analogous spring-mass system that, when the wave period is very near the natural period of the breakwater, motion and the resulting mooring forces would become large. Moorings, whether constructed of piles or mooring lines and anchors, must hold the breakwater in place and a careful assessment of mooring forces during the design storm wave attack must be made, to ensure the survival of the breakwater. Hence, to design the moorings, it is necessary to assess the motion characteristics of the floating breakwater. In addition, the breakwater unit itself must sustain the stresses imposed by wave-induced hogging and sagging, as well as those related to moorings. With regard to the structural integ-

¹Professor and Head, Dept. of Applied Mechanics and Hydraulics, National Institute of Technology Karnataka, Surathkal, Mangalore, 575025 India. E-mail: avhegde@yahoo.com

²Research Scholar, Dept. of Applied Mechanics and Hydraulics, National Institute of Technology Karnataka, Surathkal, Mangalore, 575025 India. E-mail: kiranmitin@yahoo.com

³P.G. Student, Dept. of Applied Mechanics and Hydraulics, National Institute of Technology Karnataka, Surathkal, Mangalore, 575025 India. E-mail: datta_amit@rediffmail.com

Note. Discussion open until December 1, 2007. Separate discussions must be submitted for individual papers. To extend the closing date by one month, a written request must be filed with the ASCE Managing Editor. The manuscript for this paper was submitted for review and possible publication on July 29, 2005; approved on October 27, 2006. This paper is part of the *Journal of Waterway, Port, Coastal, and Ocean Engineering*, Vol. 133, No. 4, July 1, 2007. ©ASCE, ISSN 0733-950X/2007/4-275-285/\$25.00.

urity of the breakwater unit, consideration must be given both to survival and fatigue-related stresses.

The development of floating breakwaters by various investigations has been influenced by several important features: large masses, large moment of inertia, and the combinations of two or more of the concepts of large effective mass or moment of inertia. Most of the literature indicates that the parameter "relative width" greatly influences the wave attenuation characteristics of the breakwater.

Review of Earlier Investigations on Floating Breakwaters

Homma et al. (1964) cite that the frequency response of the transmission coefficient of a floating pipe breakwater from random wave tests is essentially the same as from regular wave tests. This is due to the fact that, at higher frequency ranges, the behavior of the structure is similar in both regular and random waves. In contrast Ouellet and Morin (1975) reported that the transmission coefficient of a floating body from random wave tests was completely different from that of regular wave tests.

Harris and Webber (1968) conducted studies on a model breakwater which consisted of a floating slab of breadth comparable to the length of the wave to be attenuated. It was observed that performance was most sensitive to the area of solid slab per meter length of breakwater, but is sensitive to a lesser degree on overall breadth. They concluded that the performance [defined by $100 \times (1 - K_t)$] improved as the ratio of wavelength to solid breadth became ≤ 1 . Performance approached to 98% when the ratio of wavelength to solid breadth was 0.4.

Brebner and Ofuya (1968) conducted studies on an A frame breakwater to determine wave damping characteristics of a model floating breakwater designed to reduce incident wave heights by processes of wave reflection, wave interference, forced instability of incident waves, and turbulence. It was based on the concept that a large mass may be usefully replaced by an equivalent amount of inertia of mass. Reflection coefficients, transmission coefficients, and breakwater mooring forces were determined by experiments. For the A frame breakwater, they found that the range of effectiveness of a floating breakwater can be increased by large increase of its radius of gyration, involving only a slight increase of its mass.

Kennedy and Marsalek (1968) devised an empirical equation compatible with the wave theory and this equation was compared with the experimental results obtained for different conditions. Four box booms with porous fronts arranged in series were substituted for the model pulp-wood jam and proved to be effective in damping waves. They concluded that a flexible porous floating breakwater extending over two or more wavelengths can greatly attenuate waves of moderate length.

Chen and Wiegel (1970) designed three rigid floating breakwaters and added two more later, each making use of a different mechanism or combination of mechanisms of wave energy dissipation and reflection. The basic concept of model A was to dissipate the energy by breaking waves on a sloping board "beach." The results show that for relative width=2.7, the transmission coefficient is less than about 0.20 for Model B. Model C was a type of perforated breakwater, designed to decrease the direct striking force by decreasing the reflecting area and to dissipate wave energy by the flow of water through the holes. Model D consisted of a platform ballasted sufficiently to cause it to be immersed with its bottom beneath the water surface. Model E was

a modified version of Model D. To avoid the transmission of energy through the gates, Model E was adopted based upon the concept of a fixed energy dissipater similar to those used at the front of a spillway, rather than using the flapping gates.

Seymour (1976) suggested a program for commercial development of a tethered float breakwater for marine construction. Wave energy is attenuated through the drag produced during the rapid and vigorous oscillations of a field of buoyant spheres tethered to remain just below the surface. They indicated that the basic design variables for a deepwater tethered float breakwater are float diameter and tether length, which can be considered independently. The choice of float diameter, from a performance point of view, is a compromise between total breakwater volume and beam width.

Harms (1979) presented design curves for the Goodyear floating tire breakwater that are based on 1:4 and 1:8 scale laboratory tests, and have additionally, been substantiated by available full scale data. Two important floating tire breakwater design parameters have been assessed over a practical range of conditions, the breakwater size required for a desired level of wave attenuation and the associated peak mooring force. The experimental data for the Goodyear floating tire breakwater compared to that for the vertical plate indicate that the Goodyear floating tire breakwater with beam size equal to twelve times draft, offers approximately the same level of wave attenuation as a fixed vertical plate of equal draft. A simple mathematical model for determining transmission coefficient (K_t) was based on the assumption that power required to propel a tire of negligible mass at instantaneous velocity unidirectionally through a viscous fluid at rest is still applicable when the tire is fixed. It is further assumed that the power associated with the drag and inertia terms represents the rate at which the energy is dissipated within the structure, and that this is the dominant mechanism causing a reduction in the transmitted wave energy

$$K_t = \frac{H_t}{H_i} = \exp \left[- \frac{20\pi C_d}{3 P} \frac{\left(\frac{H_i}{L}\right)}{\left(\frac{L}{W}\right)} \right] \quad (1)$$

where H_t =transmitted wave height; H_i =incident wave height; C_d =drag coefficient; L =wavelength; W =breakwater width; and P =porosity, which is proportional to volume of breakwater by volume of tires.

Finally, it was found that the theoretical values differed from those measured by less than 10% in the region in which the breakwater provides significant wave protection, typically when $L/W < 2$.

Sastry et al. (1985) conducted an experimental investigation with a physical model of a portable tethered-float breakwater system. The performance of this system for various combinations of wave height, period, and freeboard, with the tether length kept constant, was studied. Experiments indicated that the tethered float breakwater provides effective wave attenuation when the buoys were tethered just below the still water level. The wave attenuation is closely related to wave frequency and the lowest transmission coefficient was found to be the resonant frequency of the float for any wavelength. For effective wave reduction, the beam width should be of the order of one wavelength.

Bishop (1982) made a comparative study of design curves of Harms (1979) and the Coastal Engineering Research Center (CERC). The test results of Harms (1979) and CERC were in good agreement. Further, the differences between the wave trans-

mission design curves of Harms and CERC were mainly due to model scale effects. Based on experimental and theoretical evidence, the peak mooring force design curves of Harms (1979) and CERC indicated that the dimensionless analysis of Harms (1979) is better. McCartney (1985) carried out a detailed analysis of the various types of floating breakwaters separated into four general categories of box, pontoon, mat, and tethered float. The final design is usually based on model or prototype tests of the proposed breakwater and predicted wave climate.

Leach et al. (1985) developed an analytical model to examine the response and efficiency of a rigid, hinged floating breakwater. The theoretical model has been verified experimentally and is used to develop design curves which may be employed to estimate necessary physical breakwater characteristics to satisfy attenuation criteria for specific waves. The theoretical analysis compared favorably with the experimental results. The theory shows that a hinged floating breakwater prototype of reasonable size can be designed to be an efficient wave protection device and also provides a framework for further analysis of more sophisticated structures.

A breakwater in water just over 21.32 m deep and exposed to winds blowing over a maximum fetch of 16,150 m at Bowers Harbor in Grand Traverse, Mich., was described by Sorenson (1991). The breakwater is essentially an open box 2.0 m wide, normal to the direction of wave approach, and having a draft of approximately 1.83 m. From wavelength measurements and video, the incident and transmitted wavelengths during a 15.43 m/s wind were measured. The measurements made yielded a transmission coefficient K_t of 0.21, which indicates good performance of the breakwater.

Based on the experimental and theoretical investigations on the behavior of pontoon type floating breakwaters, Sannasiraj et al. (1998) concluded that theoretical and experimental measurements show good agreement except at the roll resonance frequency. The transmission coefficient is not significantly affected by the mooring configurations studied. However, the tests showed higher transmission coefficients for a floating breakwater with cross moorings. The mooring at the water level and at the bottom of the floating breakwater yielded significantly smaller mooring forces than those obtained with crossed moorings.

Murali and Mani (1997) studied conventional floating breakwaters and the feasibility of developing a cage floating breakwater was explored. Experiments were conducted to study the performance under wave and wave-current environments. The variation of water surface oscillation and velocities within the cage, the effects of mooring line stiffness, and initial tensions on transmission characteristics are discussed. It was concluded that for a wide range of W/L (i.e., between 0.14 and 0.6), gap-to-diameter ratio equal to 0.22, relative draft of 0.46, and width of float equal to 1.0, it was possible to achieve a transmission coefficient below 0.5. The transmission coefficient increased by about 30% for waves influenced by following currents. The location or alignment of the floating breakwater should be selected so that current effects are minimal.

Sundar et al. (2003) studied the hydrodynamic performance characteristics of a floating pipe breakwater model (row of pipes separated by a distance equivalent to the pipe diameter) moored to the flume floor with a slack mooring. The investigations were carried out with random waves in an experimental program. The tests were conducted on three models with pipes of different diameter. Average reflection and transmission coefficients were evaluated as a function of relative breakwater width (W/L). Statistical analysis was carried out to prove that the heave and surge

motions, as well as peak mooring forces, follow the Rayleigh distribution.

Stiassnie and Drimer (2003) examined the suitability of a freely floating porous structure, which absorbs part of the wave energy, as a breakwater. The studies were carried out with the simplification that the motion of the box is restricted to sway only and its draft is equal to the water depth. Graphs of transmission coefficient, reflection coefficient, and energy dissipation versus wavelength to width of breakwater are plotted and compared for a porous fixed box, porous free box, and impermeable free box.

In the present paper, attempts are made to study the performance of horizontal interlaced, multilayer, moored floating pipe breakwater in the department of Applied Mechanics and Hydraulics at the National Institute of Technology Karnataka (NITK), Surathkal, Mangalore, India. This breakwater model was tested and found to be stable for storm waves of 5.4 m (18 cm model wave height, scale 1:30), which is common during the monsoon season off Mangalore coast, India. The breakwater is assumed to be flexible and intended to be economical as the material involved in its construction is polyvinyl chloride (PVC) pipes, which are relatively inexpensive and easily available compared to other materials used for the construction of the breakwaters. It can be used to create a temporary harbor area for small size boats, and to mitigate beach erosion during storm weather conditions.

Dimensional Analysis

The dimensional analysis is carried out using Buckingham's π theorem. The variables considered under the present investigations are: W =width of the breakwater; d =water depth L =wavelength; H_i =incident wave height; H_t =transmitted wave height; T =wave period; ρ =mass density; and g =acceleration due to gravity. Considering L , T , and ρ as repeating variables, the dimensional analysis yields five nondimensional π terms. These dimensionless parameters are H_t/H_i (transmission coefficient, K_t), W/L , H_i/L , d/L , and H_i/d .

Experimental Setup

The experiments were conducted in the regular wave flume of the Department of Applied Mechanics and Hydraulics, NITK, Surathkal, Mangalore, India. A sketch of the wave flume is shown in Fig. 1. The wave flume characteristics are given as

- Length=45 m;
- Width=0.75 m;
- Depth=1.0 m;
- Wave flume type=two dimensional;
- Wave generator=hinged flap type;
- Wave generated=monochromatic type; and
- Wave absorber=rubble mound spending beach.

A small wire cage with coir (made from coconut husk fiber) stuffed in it is lowered into the flume after every burst to induce quick tranquility conditions. The cage is lowered by means of a roof top pulley and a long rope, attached to the cage, as shown (not to scale) in Fig. 1. The various experimental parameters considered in the present investigations are mentioned in Table 1.

Breakwater Model

A pictorial representation of the model in plan and section views is shown in Fig. 2. The breakwater consists of PVC pipes of

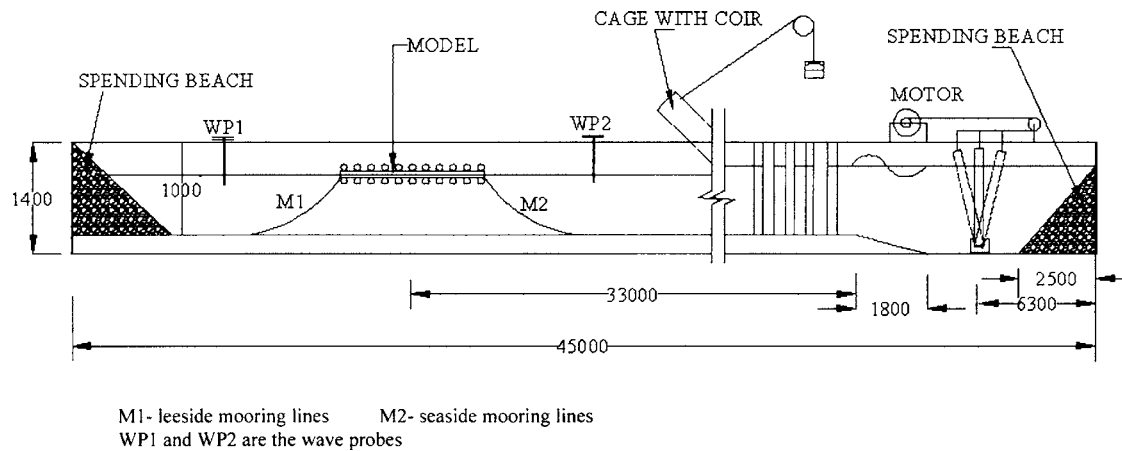


Fig. 1. Regular wave flume setup used in the present investigation (all dimensions in millimeters)

32 mm diameter. The pipes are placed parallel to each other with spacing S between them in each layer, and the adjacent layers are oriented at right angles to each other so as to form an interlacing of pipes. In the flume, longitudinal pipes are placed along the direction of propagation of waves and transverse pipes are placed and tied perpendicular to longitudinal pipes. The length of the longitudinal pipes defines the width W of the floating breakwater. It is felt that with appropriate number of layers n , spacing of pipes S , and relative breakwater width W/L , it is possible to achieve a considerable and effective attenuation of waves.

In the present work, regular waves of periods mentioned in Table 1 were generated for W/L ratios of 0.4–1.2. The depths of water considered were 400, 450, and 500 mm. A spacing to di-

ameter ratio $S/D=5$ was used. Three layers were used (two transverse and one longitudinal). Based on the W/L ratios used, the range of breakwater widths were from 0.77 to 4.91 m. Waves were generated in bursts of five waves only to avoid distortion due to reflection and re-reflection from the breakwater structure and the wave paddle. After the burst, wave generation was stopped until tranquility was achieved in the flume. Thereafter, the next burst of five waves was generated. For each run, six trials were conducted and the average of the six values of transmitted wave height was recorded and used to compute the transmission coefficient for that particular run. Linear capacitance type wave gauges, along with amplification units, were used for acquiring water surface elevations in the wave flume.

Scale Factor. The floating breakwater described in this paper is modeled to suit a prototype maximum wave height of 6 m. A geometrically similar scale of 1:30 was adopted and hence, the range of model wave heights was 30–180 mm.

Table 1. List of Different Experimental Parameters

Water depth, d (mm)	Number of layers, n	Ratio of spacing to diameter, S/D	Wave period, T (s)	Incident wave height, H_i (mm)	Relative width of breakwater (W/L)
400, 450, and 500	3	5	1.2	60	0.4,
				90	0.5,
			1.4	60	0.6,
				90	0.7,
			1.6	120	0.8,
				90	0.9,
	2.0	3	1.8	60	1.0,
				90	1.1,
			2.0	120	1.1,
				120	and
			2.2	60	1.2
				90	
500	3	5	1.8	120	
				150	
			2.0	180 ^a	
				120	
			2.2	60	
				120	
	150				
	180 ^a				

^a180 mm wave height is generated only for 500 mm depth of water.

Results and Discussion

The experiments were conducted for number of layers, $n=3$; depths of 400, 450, and 500 mm; wave heights ranging from 30 to 180 mm; and wave periods ranging from 1.2 to 2.2 s.

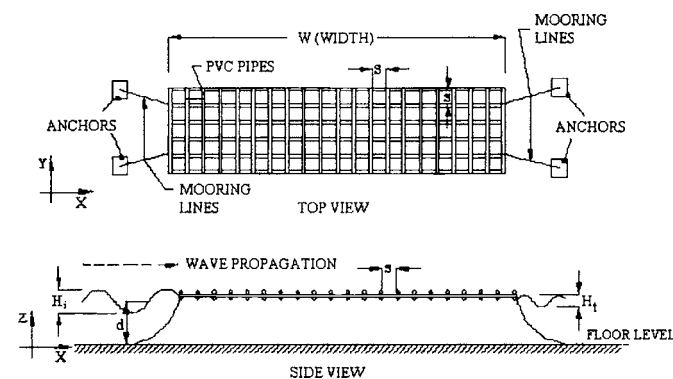


Fig. 2. Floating pipe breakwater model setup used in the present work

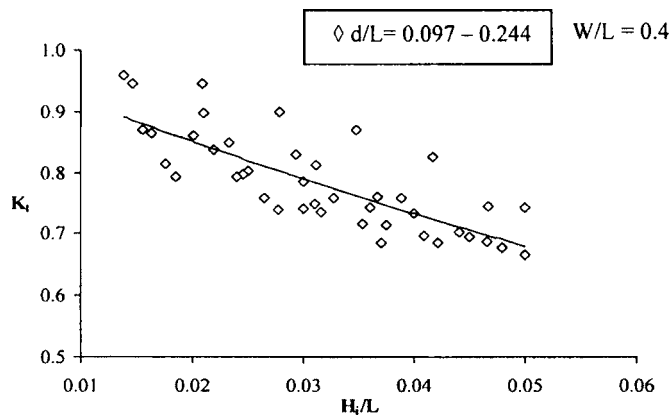


Fig. 3. Variation of transmission coefficient versus wave steepness for a range of d/L values and $W/L=0.4$

Variation of K_t with Relative Wave Steepness H_i/L

Figs. 3–10 show the variation of transmission coefficient K_t with wave steepness H_i/L for values of relative water depth d/L ranging from 0.097 to 0.244, and different relative breaker widths W/L . The lines on these plots are the least squares exponential fit to the data. It may be noted from Figs. 3–10 that as steepness increases, K_t decreases. In other words, steep waves are found to

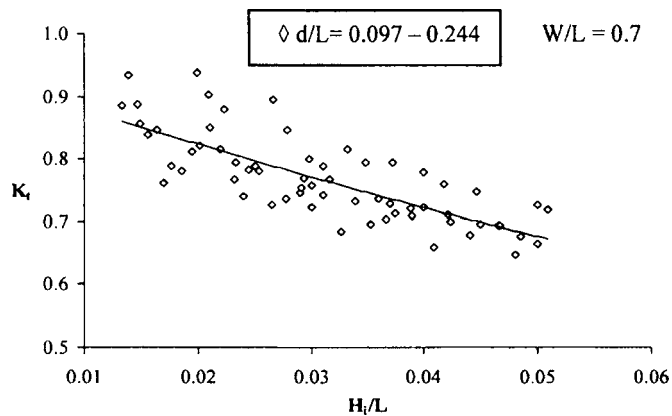


Fig. 6. Variation of transmission coefficient versus wave steepness for a range of d/L values and $W/L=0.7$

undergo greater attenuation than those with smaller steepness. This tendency is obvious because, as steepness increases, the wave heights are large (and wavelengths are short), the waves tend to become sharp-crested and hence become unstable. As these steep waves meet an obstruction, a large amount of energy is dissipated due to instability and hence more attenuation of wave height is achieved. For waves of low steepness (small wave heights, larger wavelengths), the instability does not occur, energy

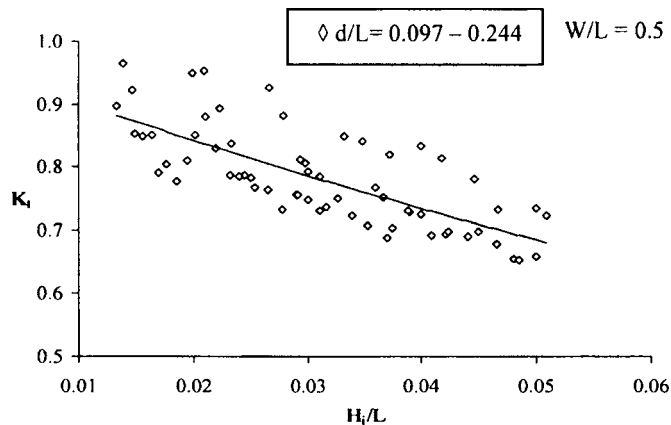


Fig. 4. Variation of transmission coefficient versus wave steepness for a range of d/L values and $W/L=0.5$

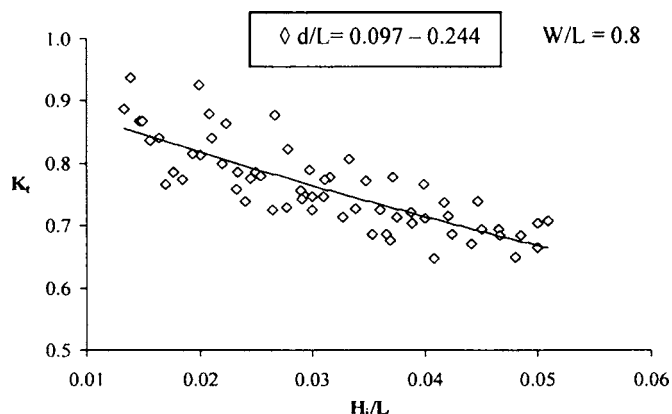


Fig. 7. Variation of transmission coefficient versus wave steepness for a range of d/L values and $W/L=0.8$

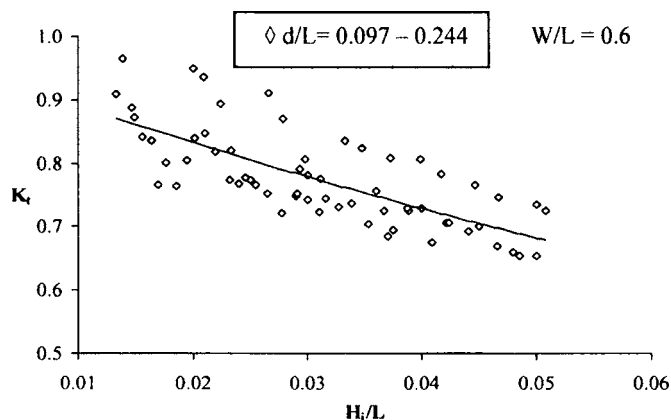


Fig. 5. Variation of transmission coefficient versus wave steepness for a range of d/L values and $W/L=0.6$

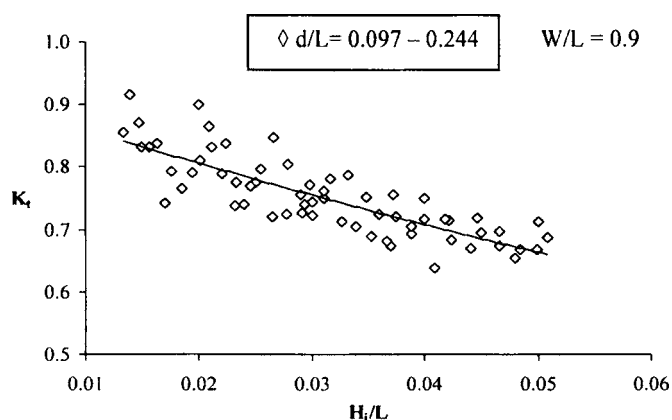


Fig. 8. Variation of transmission coefficient versus wave steepness for a range of d/L values and $W/L=0.9$

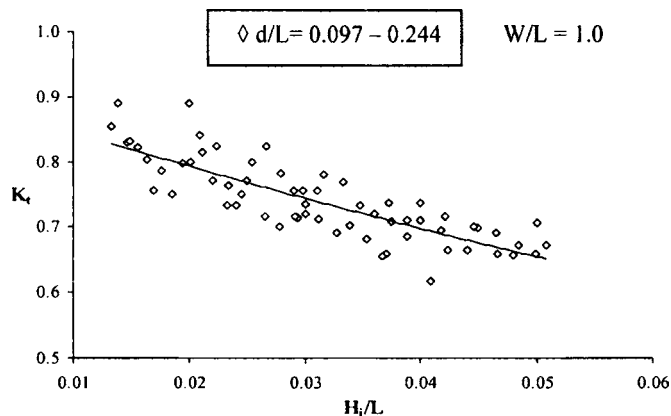


Fig. 9. Variation of transmission coefficient versus wave steepness for a range of d/L values and $W/L=1.0$

dissipation is less, and attenuation is small. This observation is in agreement with earlier investigators as reported by Brebner and Ofuya (1968), Harms (1979), Sastry et al. (1985), and Murali and Mani (1997).

Figs. 4–7 are plotted for various values of $W/L=0.5–0.8$. It may be noted that the maximum attenuation taking place for these cases is limited to 34% for the previous W/L values and for all H_i/d and d/L values. This information may be used for arriving at appropriate values of W/L for attaining required attenuation.

Variation of K_t with Relative Breakwater Width W/L

Relative width (W/L) of the breakwater plays a significant role in wave transmission characteristics, because of viscous as well as turbulent dissipation of wave energy as the waves propagate past the breakwater. The variation of transmission coefficient with the variation in relative breakwater width, W/L , for different relative wave height, H_i/d , and wave steepness, H_i/L , is shown in Figs. 11–24. It is observed from these figures that the transmission coefficient K_t decreases with increasing relative breakwater width, in general. This is due to the fact that, for a given wavelength, as W/L increases, the width of the breakwater increases and a large amount of wave structure interaction takes place which results in greater wave attenuation.

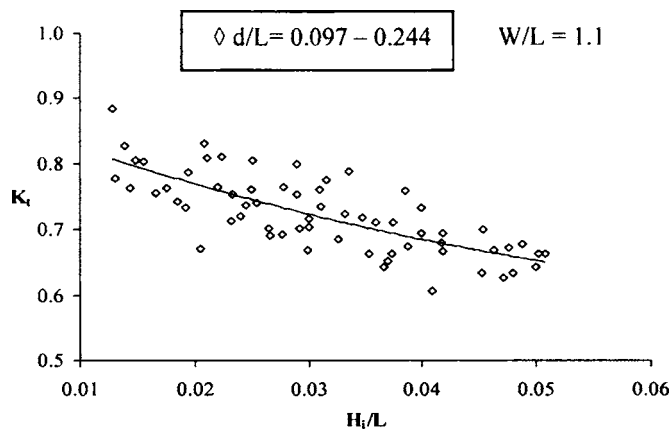


Fig. 10. Variation of transmission coefficient versus wave steepness for a range of d/L values and $W/L=1.1$

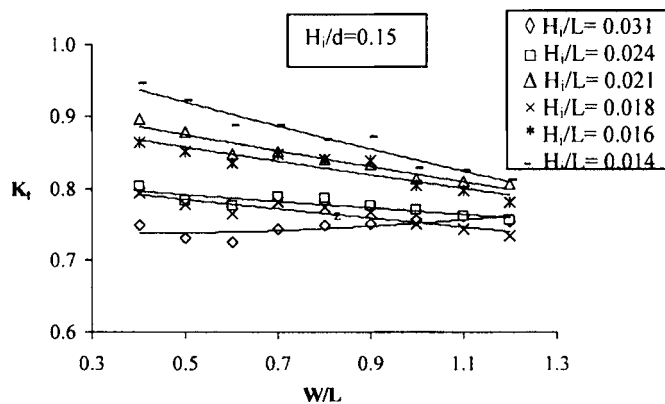


Fig. 11. Variation of transmission coefficient versus relative breakwater width for $H_i/d=0.15$

It may be noted that for $H_i/L=0.024$ (Figs. 11–13 and 15), W/L has very low or no influence on K_t . However, for $H_i/L=0.031$ (Figs. 11–13 and 17) with an increase in W/L value, a slight increase in K_t is observed. This may be explained as follows: Waves transmitted by a floating breakwater are the aggregate result of a complex hydrodynamic interaction between the floating breakwater and the incident wave field. As previously stated, a portion of the incident wave energy is reflected by the structure and some energy passes under (and over) the breakwater. Further, a portion of the incident wave field excites a small

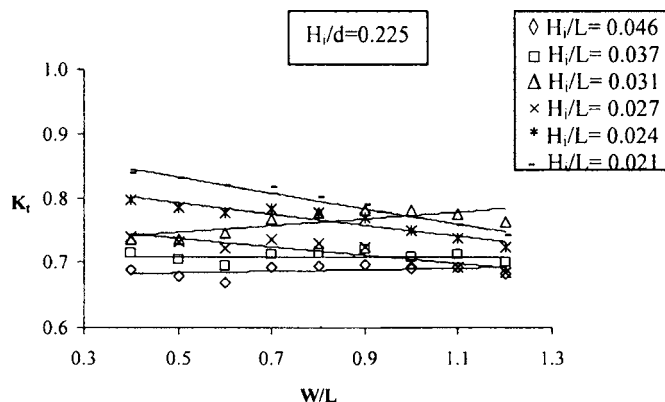


Fig. 12. Variation of transmission coefficient versus relative breakwater width for $H_i/d=0.225$

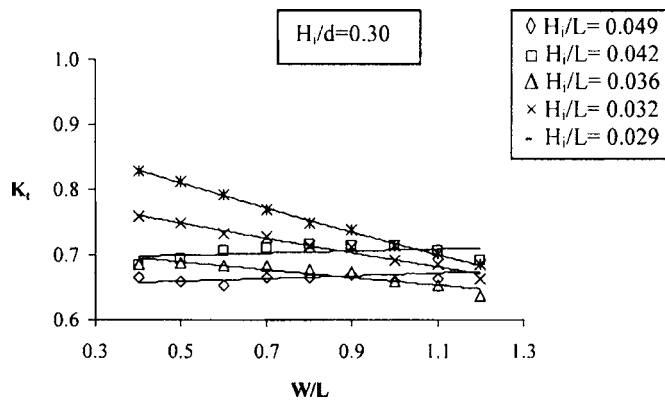


Fig. 13. Variation of transmission coefficient versus relative breakwater width for $H_i/d=0.30$

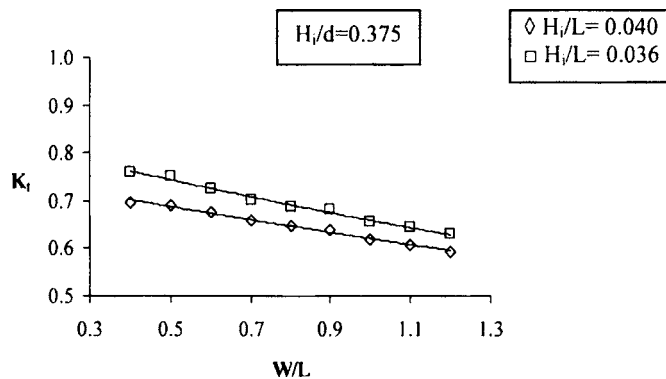


Fig. 14. Variation of transmission coefficient versus relative breakwater width for $H_i/d=0.375$

motion of the anchored floating breakwater, which in turn, generates small waves in a manner similar to the wavemaker in a physical hydraulic model. The total transmitted wave is the sum of components that pass under (and over) the breakwater and components that are generated by breakwater motion. For $H_i/L=0.031$, the wave generated by motion of the breakwater may be in phase with the incident waves and hence an increase in K_t would have occurred. Fig. 12 shows almost a similar trend, as observed in Fig. 11. It is interesting to note that for $H_i/L=0.031$, there is an increase in K_t with the increase in W/L , but for higher

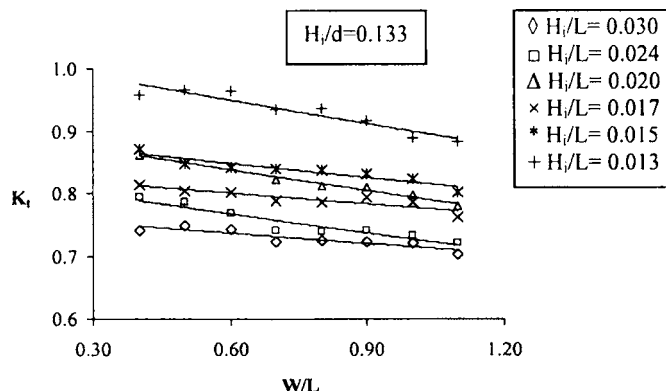


Fig. 15. Variation of transmission coefficient versus relative breakwater width for $H_i/d=0.133$

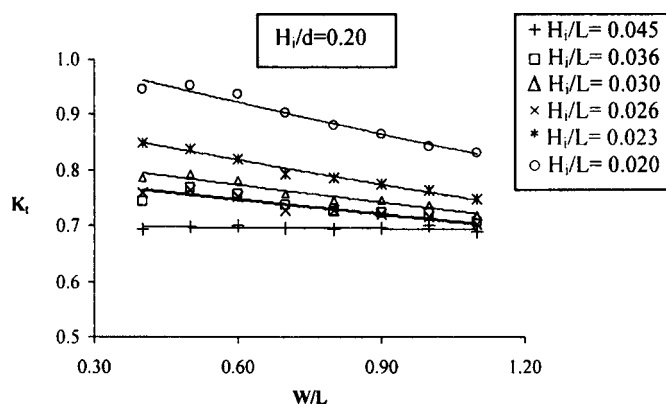


Fig. 16. Variation of transmission coefficient versus relative breakwater width for $H_i/d=0.20$

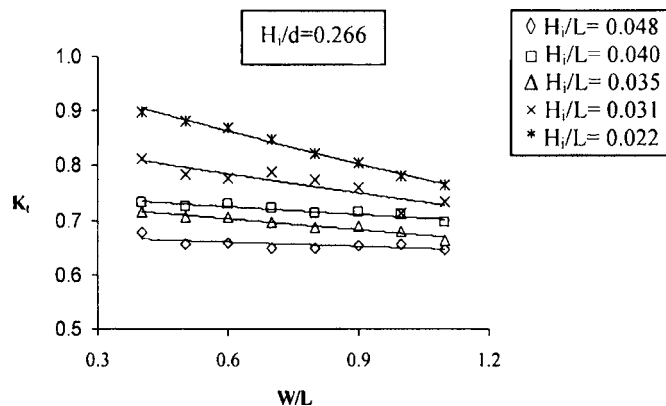


Fig. 17. Variation of transmission coefficient versus relative breakwater width for $H_i/d=0.266$

values of H_i/L (≥ 0.037) the influence of W/L on K_t is almost insignificant for this particular wave height. Fig. 13 shows similar trends as observed in Fig. 12.

It is interesting to note that for $H_i/L=0.042$ (Fig. 23), there is an increase in K_t with increase in W/L , but for $H_i/L=0.049$ the influence of W/L on K_t is almost insignificant. In Fig. 14, a decreasing trend with an increase in W/L may be observed. For the high H_i/L values (0.036 and 0.040), only a slight decrease in K_t (about 5%) is observed over the range of W/L values. The previous graphs cite the fact that for relative wave heights H_i/d of 0.15

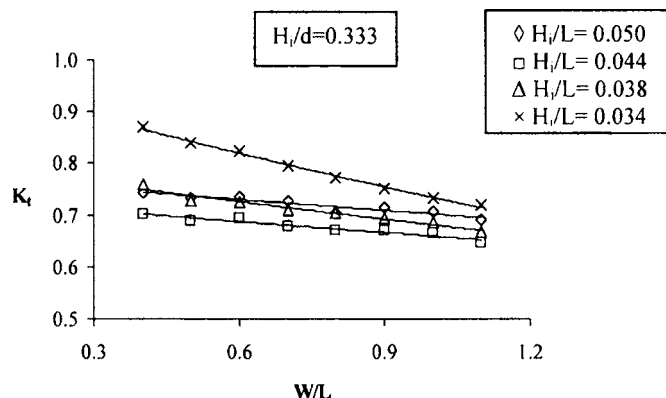


Fig. 18. Variation of transmission coefficient versus relative breakwater width for $H_i/d=0.333$

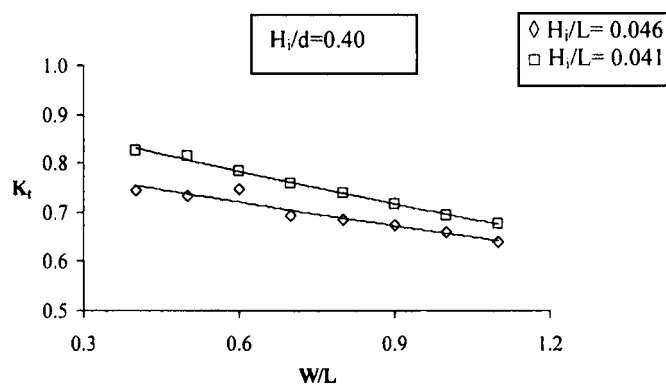


Fig. 19. Variation of transmission coefficient versus relative breakwater width for $H_i/d=0.40$

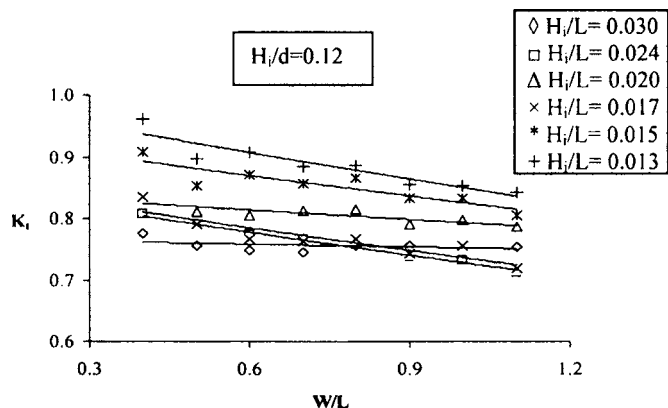


Fig. 20. Variation of transmission coefficient versus relative breakwater width for $H_i/d=0.12$

and 0.225 (Figs. 11 and 12), K_t values decrease with an increase in W/L ratio and at a critical value of $H_i/L=0.031$, K_t increases with the increase in W/L ratio. For values of H_i/L beyond this critical value, there is no significant effect of W/L on K_t . For relative wave height $H_i/d=0.3$, the critical $H_i/L=0.042$. From the graphs it can also be cited that as H_i/d increases, K_t decreases. For $H_i/d=0.15$ (Fig. 11) the minimum observed K_t value was 0.72, which reduced dramatically to 0.6 for $H_i/d=0.375$ (Fig. 11). This indicates that with an increase in wave heights, the relative

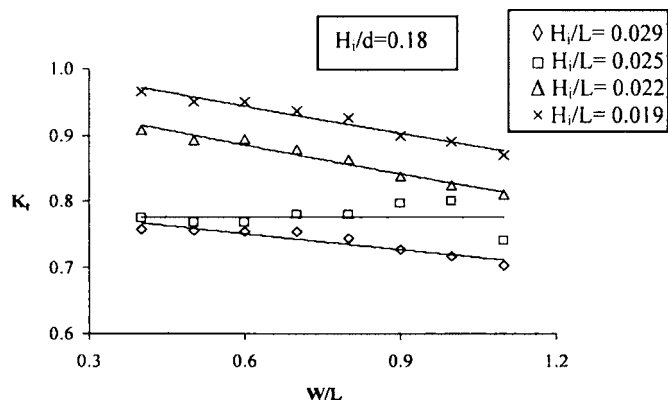


Fig. 21. Variation of transmission coefficient versus relative breakwater width for $H_i/d=0.18$

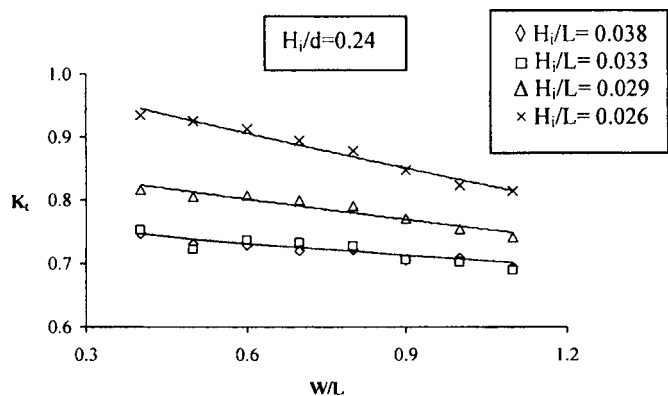


Fig. 22. Variation of transmission coefficient versus relative breakwater width for $H_i/d=0.24$

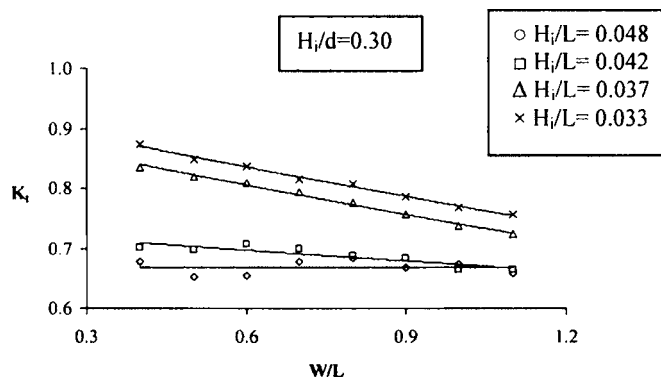


Fig. 23. Variation of transmission coefficient versus relative breakwater width for $H_i/d=0.30$

wave height tends toward the breaking limit of the wave ($H_b=0.78d$) where turbulence creates greater attenuation of the waves. Similar types of graphs are also shown for $H_i/d=0.133-0.4$ and $H_i/d=0.12-0.36$ (water depths of 450 and 500 mm) in Figs. 15–24, respectively.

Fig. 15 shows the variation of K_t and W/L as a function of H_i/L for $H_i/d=0.133$ (depth, $d=450$ mm and $H_i=60$ mm). It can be seen that K_t decreases with an increase in W/L . In this graph it can be easily observed that the low steepness waves undergo less attenuation as they are more stable, whereas the high steepness waves experience greater attenuation as the effect of W/L on K_t is much less.

Fig. 16 indicates a similar trend of decreasing K_t with increasing W/L values. However, it may also be observed that for $H_i/L=0.045$ the influence of W/L on K_t is insignificant. The same trend is evident in Fig. 17 for $H_i/L=0.048$. Hence for $d=450$ mm, it may be observed that a decreasing trend is observed for all the wave steepness values, and for $H_i/L=0.045$ and $H_i/L=0.049$ the effect of W/L on K_t is insignificant. From Figs. 15–19, the same decreasing trend of K_t with the increase in H_i/d values is observed.

From Figs. 20–24, it is inferred that there is no significant influence of W/L on K_t for $H_i/L=0.025$, 0.03, and 0.0485. In addition, from the graphs in Figs. 11–24, it may also be concluded that H_i/d is also an influencing parameter in the performance of floating pipe breakwaters.

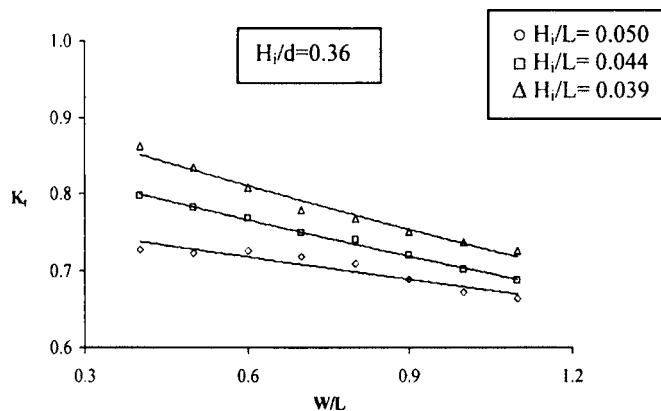


Fig. 24. Variation of transmission coefficient versus relative breakwater width for $H_i/d=0.36$

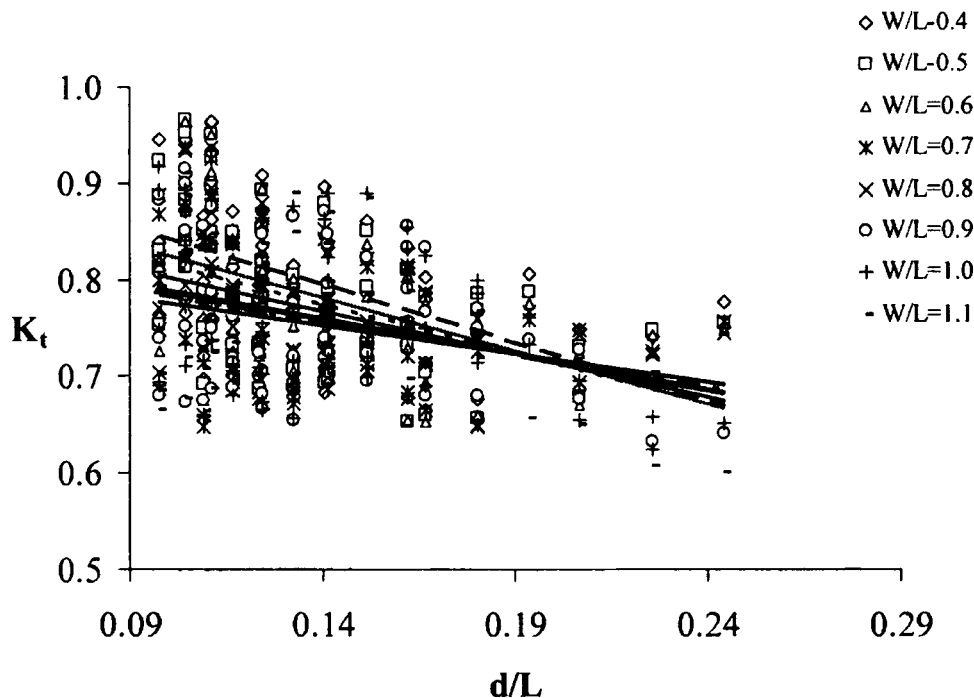


Fig. 25. Variation of transmission coefficient versus relative depth for different values of W/L

Variation of K_t with Relative Water Depth d/L

The relative water depth (d/L) is the deciding factor in determining shallow, intermediate, and deepwater wave conditions. As water particle velocity and orbital motion change with depth, this factor becomes more dominant in influencing the wave attenuating characteristics of the structure.

The relative depth d/L in the present experiments was varied from 0.244 to 0.097. However, this corresponds to intermediate depth conditions. Graphs are plotted for d/L versus K_t as a function of W/L in Fig. 25. Referring to Fig. 25, it is seen that K_t decreases with an increase in d/L . This tendency can be attributed to the fact that as d/L tends toward deep waters, energy is concentrated more at the surface, which is better dissipated by the floating breakwater. In shallow waters (i.e., $d/L \leq 0.05$), the distribution of energy is more or less uniform with more passing below the floating breakwater.

Comparison with Harms (1979) Mathematical Model

The power required to propel a tire (of negligible mass) at a velocity, unidirectionally through a viscous fluid, is the basic principle used in the Harms (1979) mathematical model. It is assumed that this basic relationship is still applicable, when the tire is fixed and the velocity is the instantaneous velocity of an external current, even when this flow is not only unsteady but also periodically reversing, such as generated by the action of water waves. Considering the case of a floating breakwater, made almost entirely of automobile tires, it was assumed that the power associated with the drag and inertia terms represents the rate at which energy is dissipated within the structure, and that this is the dominant mechanism causing a reduction in the transmitted wave energy. Parameter P is defined to serve as a measure of porosity of the breakwater. The rate of energy dissipation within a segment of the breakwater is assumed to be proportional to the number of

tires contained in that segment. Using linear wave theory, the average rate at which the wave energy is transported is considered across a section of the breakwater.

If the velocity field within the breakwater can be correctly specified, then the variation of wave height along the beam of the breakwater can be obtained from above principles. But, this is a difficult task, since the structure is not small compared to the incident wavelength, so that the pure (no structure) wave-induced flow field is probably a poor approximation to the actual flow field within and around the breakwater. In view of the complexity of the flow field within the structure (wave breaking, splashing, air entrainment, surging, etc.), which cannot be accounted for even in most of the sophisticated wave theories, Harms (1979) deemed that linear wave theory and deep water conditions (i.e., $d/L > 0.5$) were adequate as first approximations.

The results obtained from the present experiments were compared with Harms (1979) mathematical model. It was found that (Tables 2 and 3 and Fig. 26), for $H_i/L = 0.04$, the transmission coefficients as obtained by the model of Harms (1979) and those obtained from present experimental results agreed satisfactorily for $W/L > 0.6$. The theoretical values obtained by Harms model differ from the present values by less than 10% for $W/L > 0.6$. The maximum deviation of $\pm 15\%$ was observed over the range of values of W/L and H_i/L considered in the experiments. The sway motion of the breakwater was assumed negligibly small in the Harms model, which is valid for short waves $W/L \geq 1$, and it becomes increasingly inappropriate in the region $W/L \leq 1$.

For each W/L value tested, the appropriate value of C_d/P was determined from Eq. (1) by considering the theoretical and experimental value of K_t as follows: The values of d , H_i/L , porosity parameter P , and K_t obtained from experimental results for $W/L = 1.0$ were substituted in Eq. (1) and corresponding C_d/P values were computed. The C_d/P values computed were substituted back in Eq. (1) and K_t values were calculated for various

Table 2. K_t Values Obtained from Experiments for $H_i/L \approx 0.04$

W/L	K_t values for different W/L values and depth				
	$d=400$ mm $H_i/L=0.040$	$d=450$ mm $H_i/L=0.04$	$d=450$ mm $H_i/L=0.041$	$d=500$ mm $H_i/L=0.0388$	$d=500$ mm $H_i/L=0.0399$
0.4	0.6973	0.7331	0.8268	0.7463	0.8616
0.5	0.6914	0.7251	0.8135	0.7311	0.8333
0.6	0.6759	0.7293	0.7832	0.7288	0.8075
0.7	0.6592	0.7230	0.7589	0.7206	0.7790
0.8	0.6477	0.7121	0.7379	0.7210	0.7670
0.9	0.6391	0.7164	0.7170	0.7047	0.7503
1.0	0.6179	0.7104	0.6949	0.7093	0.7363
1.1	0.6070	0.6955	0.6776	0.6936	0.7259
1.2	0.5935	—	—	—	—

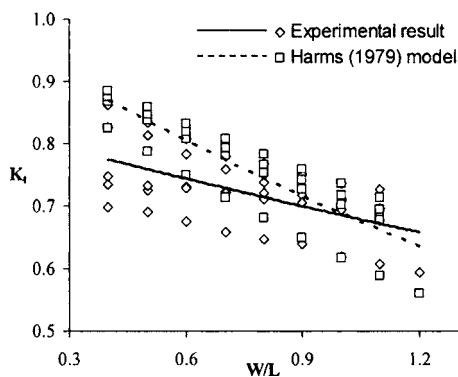
Table 3. K_t Values Computed by Harms (1979) Mathematical Model for $H_i/L \approx 0.04$

W/L	K_t values for different W/L values and depth				
	$d=400$ mm $H_i/L=0.040$ $C_d/P=0.57$	$d=450$ mm $H_i/L=0.04$ $C_d/P=0.40$	$d=450$ mm $H_i/L=0.041$ $C_d/P=0.43$	$d=500$ mm $H_i/L=0.0388$ $C_d/P=0.40$	$d=500$ mm $H_i/L=0.0399$ $C_d/P=0.364$
0.4	0.6925	0.7337	0.8206	0.7463	0.8621
0.5	0.6866	0.7257	0.8068	0.7311	0.8340
0.6	0.6710	0.7299	0.7756	0.7288	0.8083
0.7	0.6540	0.7237	0.7507	0.7206	0.7798
0.8	0.6424	0.7127	0.7290	0.7210	0.7679
0.9	0.6337	0.7170	0.7076	0.7047	0.7515
1.0	0.6123	0.7111	0.6849	0.7093	0.7373
1.1	0.6013	0.6962	0.6672	0.6936	0.7270
1.2	0.5877	—	—	—	—

W/L values. The value of the porosity parameter P is constant for all values of the width of the breakwater, as the parameter S/D was kept at a constant value of 5, throughout the experiments in the present work. The C_d/P values were computed for different depths of water, as it is a function of wavelength and hence depth of water.

Conclusions

1. The transmission coefficient K_t decreases with the increase in wave steepness H_i/L for all W/L and d/L values.

**Fig. 26.** Comparison of K_t values computed by Harms (1979) mathematical model with that from present experiments

2. Low steepness waves approximately up to 0.02 pass through the breakwater without much attenuation. A maximum attenuation of up to 10% was observed.
3. The transmission coefficient K_t decreases with the increase in relative breakwater widths W/L for all H_i/d values considered.
4. The transmission coefficient K_t is not influenced by W/L for H_i/L values between 0.027 and 0.031 for $H_i/d=0.15-0.375$. For $H_i/L=0.031$, $H_i/d=0.15$, and $H_i/d=0.225$ increase in K_t is observed (3–5%) with the increase in W/L. For $H_i/L=0.042$ and $H_i=120$ mm, an increase in K_t value of about 3% is observed.
5. For $H_i/d=0.12-0.40$, the influence of W/L on K_t is insignificant for $H_i/L < 0.030$ and $H_i/L > 0.0485$ and the major attenuation takes place between the values of $H_i/L=0.03$ to 0.0485.
6. The maximum wave attenuation achieved in the present study is 40.5% for W/L=1.0 and $H_i/d=0.3$.
7. For $H_i/L=0.04$, the mathematical model by Harms (1979) and those obtained from present experimental results are in agreement with each other. However, for other values of H_i/L a maximum deviation of $\pm 15\%$ from the experimental values were observed.

Acknowledgments

The writers would like to express their sincere thanks to the Director, National Institute of Technology Karnataka, Surathkal,

Mangalore, India, for providing all the necessary infrastructural facilities for the present study.

Notation

The following symbols are used in this paper:

- C_d = drag coefficient;
 D = diameter of pipes;
 d = still water depth;
 d/L = relative depth;
 g = acceleration due to gravity;
 H_i = incident wave height;
 H_i/d = relative wave height;
 H_i/L = relative wave steepness;
 H_t = transmitted wave height;
 K_t = transmission coefficient;
 L = wavelength;
 n = number of layers of pipes;
 P = porosity;
 S = spacing between the pipes;
 S/D = ratio of spacing to diameter of pipes;
 T = time period of waves;
 W = width of the breakwater; and
 W/L = relative breakwater width.

References

- Bishop, C. T. (1982). "Floating tire breakwater design comparison." *J. Waterway, Port, Coast., and Oc. Div.*, 108(3), 421–426.
- Brebner, A., and Ofuya, A. O. (1968). "Floating breakwaters." *Proc., 11th Coastal Engineering Conf.*, ASCE, London, 1055–1094.
- Chen, K., and Wiegel, R. L. (1970). "Floating breakwaters for reservoir marinas." *Proc., 12th Coastal Engineering Conf.*, ASCE, Vol. III, Washington, D.C., 1647–1666.
- Harms, V. W. (1979). "Design criteria for floating tire breakwaters." *J. Waterway, Port, Coast., and Oc. Div.*, 105(2), 149–170.
- Harris, A. J., and Webber, N. B. (1968). "A floating breakwater." *Proc., 11th Coastal Engineering Conf.*, ASCE, London, 1049–1054.
- Homma, M., Horikawa, K., and Mochizuki, H. (1964). "An experimental study of floating breakwaters." *Int. Conf. on Coastal Engineering, Japan*, JSCE, Vol. 7, 85–94.
- Kennedy, R. J., and Marsalek, J. (1968). "Flexible porous floating breakwater." *Proc., 11th Coastal Engineering Conf.*, ASCE, London, 1095–1103.
- Leach, P. A., McDougal, W. G., and Sollitt, C. K. (1985). "Hinged floating breakwater." *J. Waterway, Port, Coastal, Ocean Eng.*, 111(5), 895–909.
- McCartney, B. L. (1985). "Floating breakwater design." *J. Waterway, Port, Coastal, Ocean Eng.*, 111(2), 304–318.
- Murali, K., and Mani, J. S. (1997). "Performance of cage floating breakwater." *J. Waterway, Port, Coastal, Ocean Eng.*, 123(4), 172–179.
- Ouellet, Y., and Morin, Y. (1975). "Effect of structures on irregular waves compared to regular waves." *J. Waterway, Port, Coastal, Ocean Eng.*, 101(3), 231–246.
- Sannasiraj, S. A., Sundar, V., and Sundaravadivelu, R. (1998). "Mooring forces and motion response of pontoon-type floating breakwaters." *Ocean Eng.*, 25(1), 27–48.
- Sastry, J. S., Narasimhan, S., and Vethamony, P. (1985). "Model studies on tethered float breakwater system." *Proc., 1st National Conf. on Dock and Harbor Engineering*, IIT Bombay, Mumbai, Vol. 2, E273–E286.
- Seymour, R. J. (1976). "Tethered float breakwaters: A temporary wave protection system for open ocean construction." *Proc., Offshore Technology Conf.*, Dallas, 253–258.
- Sorenson, M. R. (1991). "Discussion of 'Floating breakwater for small recreational harbors' by J. E. Muschell and J. H. Schlak." *J. Waterway, Port, Coastal, Ocean Eng.*, 117(5), 427–428.
- Stiassnie, M., and Drimer, N. (2003). "On a freely floating porous box in shallow water waves." *Appl. Ocean Res.*, 25(5), 263–268.
- Sundar, V., Sundaravadivelu, R., and Purushotham, S. (2003). "Hydrodynamic characteristics of moored floating pipe breakwater in random waves." *Proc., Institution of Mechanical Engineers, Part M: J. Engrg. Maritime Environment*, 217(M), 95–110.